Experimental Brain Research (2021) 239:3573–3583
https://doi.org/10.1007/s00221-021-06231-4

RESEARCH ARTICLE

Low-cost brain computer interface for everyday use

Ildar Rakhmatulin[1] · Andrey Parfenov[2] · Zachary Traylor[3] · Chang S. Nam[3] · Mikhail Lebedev[4]

Received: 27 June 2021 / Accepted: 21 September 2021 / Published online: 29 September 2021

Abstract

With the growth in electroencephalography (EEG) based applications *the demand for affordable consumer solutions is increasing*. Here we describe a compact, low-cost EEG device suitable for daily use. *The data are transferred* from the device to a personal server using the TCP-IP protocol, *allowing for wireless operation* and a decent range of motion for the user. The device is compact, having a circular shape with a radius of only 25 mm, which would allow for comfortable daily use during both daytime and nighttime. Our solution is also very cost effective, approximately $350 for 24 electrodes. *The built-in noise suppression capability* improves the accuracy of *recordings with a peak input noise below 0.35 μV*. Here, we provide the results of the tests for the developed device. On our GitHub page, we provide detailed specification of the steps involved in building *this EEG device which* should be helpful to readers designing similar devices for their needs https://github.com/Ildaron/ironbci.

Keywords Brain computer interface (BCI) · EEG · Signal processing · ironbci · Low-cost BCI · Low-cost EEG

Introduction

Electroencephalography (EEG) is one of the most popular methods for researching the brain; it functions via recordings of neural activity using the electrodes placed on a subject's scalp. The information obtained via EEG is used for various purposes, including research and clinical applications. Many manuscripts in the field of EEG signal processing even attempt to diagnose diseases with the use of information received from EEG electrodes. For example, Kanda et al. (2017) used the alpha rhythm of the brain (7–13 Hz signals) to improve the discrimination of mild Alzheimer's disease. Tylová et al. (2018) used an unbiased estimation of permutation entropy for EEG analysis. Yu et al. (2018) used the permutation disalignment index to research the functional brain connectivity in Alzheimer's disease patients. More recently, Asadzadeh et al. (2020) presented a complete review of brain pathologies based on EEG signals and source localization.

Various types of electrode sensors can be used to "measure EEG signals, including but not limited to wet, contact, and non-contact". The highest quality signal is usually obtained with disposable wet sensors due to their low impedance: in some systems as high as 200 kOhm before applying the "wet" conductive gel and as low as 5 kOhm after applying the gel (Lopez-Gordo 2014). One disadvantage of using wet electrodes, however, is the impedance drift as the gel dries, which introduces significant changes in the measured signal. The usage of electrode gel also requires a great deal of set-up time, and results in the patient needing to wash the gel out of their hair after the experiment. Obtaining an EEG signal with a dry contact electrode on the other hand is a more comfortable way to obtain information about the functioning of the human brain, as it avoids the mess of the electrode gel and the set-up/take-down time associated with cleaning the electrodes and the participant. Unfortunately, this method is not the most reliable and not suitable for all scenarios. A relatively high-contact impedance, due to insufficient electrical connection at the electrode–scalp interface,

Communicated by Bill J Yates.

✉ Ildar Rakhmatulin
ildar.o2010@yandex.ru

[1] South Ural State University, Chelyabinsk, Russia

[2] Brainflow, Moscow, Russia

[3] Edward P. Fitts Department of Industrial and Systems Engineering, North Carolina State University, Raleigh, NC, USA

[4] Skolkovo Institute of Science and Technology, Moscow, Russia

remains the main problem that hinders the widespread use of dry electrodes over wet ones (Lopez-Gordo 2014).

The relevance of the development of a low-cost device for measuring EEG signals is confirmed by many works in this area in which authors utilized inexpensive commercial devices. Gunawan and Surya (2018) used an Emotiv EEG headset with 14 electrodes (about $ 1000) to classify brain waves based on an EEG spectrogram. Using the same equipment, Ashby et al. (2011) performed a simple motor imagery experiment, common in BCI designs, where the subject imagined moving their limbs. A common disadvantage of these devices, however, is the lack of flexibility in use. The Emotiv device is not open source and thus, there is no way to make edits to the firmware itself. Low measurement quality and non-compliance with international standards for the location of electrodes [10–20 system (Chatrian 1985)] can also lead to issues in replication when utilizing the Emotiv EEG headset.

Today, one of the most popular devices for measuring EEG signals in the low-cost segment is the biosensing device from OpenBCI (https://openbci.com/), but its costs still exceed $1000 for a 16-channel setup. Peterson et al. (2020) experimentally investigated this board and found that the quality of the EEG signal was not always good enough for highly accurate EEG recordings. These issues could possibly be related to the fact that the board has no isolation from external magnetic fields, however this could just as well be explained by other conditions in the room. Chaudhary et al. (2016) and Luis et al. (2012) came to similar conclusions in their works, in which they compared low-cost devices for measuring EEG signals. These problems with the quality are to be expected, as many of the devices from the low-cost series are marketed as entertainment devices rather than research-grade equipment. Regarding research into "DIY" research-aimed EEG devices, Senevirathna et al. (2016) measured seven EEG channels paired with one audio channel and transmitted these data to an external device via Bluetooth. This study was a typical implementation of the Texas Instruments ADS1299 analog to digital converter (ADC). However, the board was not compact, the possibility of autonomous use was not considered, and authors did not present information on the quality of the EEG signal (i.e. amount of noise). Similar disadvantages are found in Graham et al. (2014), where the process was described in detail for developing a compact, low-cost wireless EEG device. Tyler et al. (2015) also described the development of a device for reading EEG signals, however, there is no information about the manufacturer of the components, the layout of the printed circuit board, or the PCB board characteristics. In a paper that addressed similar issues as we examine here, Uktveris and Jusas (2018) considered both ADS1299 and the ADS1288 ADCs. The board presented in their work had only the standard implementation recommended by the manufacturer for the ADC, one aimed at the Arduino market as an additional shield for the MEGA2560 models. Therefore, this board is less suitable for studying EEG signals and more focused on merely acquiring them. Also, the manuscript provides no information about the equipment that was used to test the developed device for noise, a subject we cover in more detail here.

A promising application of a low-cost yet functional EEG device is the possibility of its use as part of a brain–computer interface (BCI). BCIs are used in various fields, with the most important goal being helping people with disabilities. BCI devices, through the conversion of signals from the brain into instructions for a computer, allow disabled subjects to control various actuators and enable actions they have difficulty performing. A more affordable EEG device would directly allow the development of affordable BCI devices for these individuals. This would also help promote new research in the field, as current, high-quality EEG systems are often expensive (as mentioned later in this paper). At the same time, BCI technologies still have several problems that limit their development, several of which Kübler described in her paper (Kübler 2007). These include the limited number of brain signals understood well enough to be used in applications and the need for re-calibration of the signal processing algorithms every single session. Furthermore, many BCI devices use machine learning to classify brain signals out of EEG data, and this process requires substantial amounts of consistent data with few uncontrolled artifacts (Savadkoohi et al. 2020; Dadebayev et al. 2021). To accomplish this feat, the field needs a compact device that works unsupervised for extended periods of time while wirelessly transmitting the recorded signals for signal processing.

This paper presents a device for reading EEG signals with a focus on lower cost, higher accuracy, and advanced functionality. This work is distinguished by technical decisions made to improve the accuracy and quality of the EEG measurements needed for traditional EEG studies as well as BCI experiments and designs. We discuss the most important decisions, such as the selection of the ADC, in this paper while specific steps to produce the device can be found on the GitHub page. We set out to develop a compact device with low power consumption and accuracy comparable to that of laboratory instruments. The block diagram of our proposed device is shown in Fig. 1: demonstrating how the STM32 microcontroller receives signals and transmits them to the computer via different types of adapters.

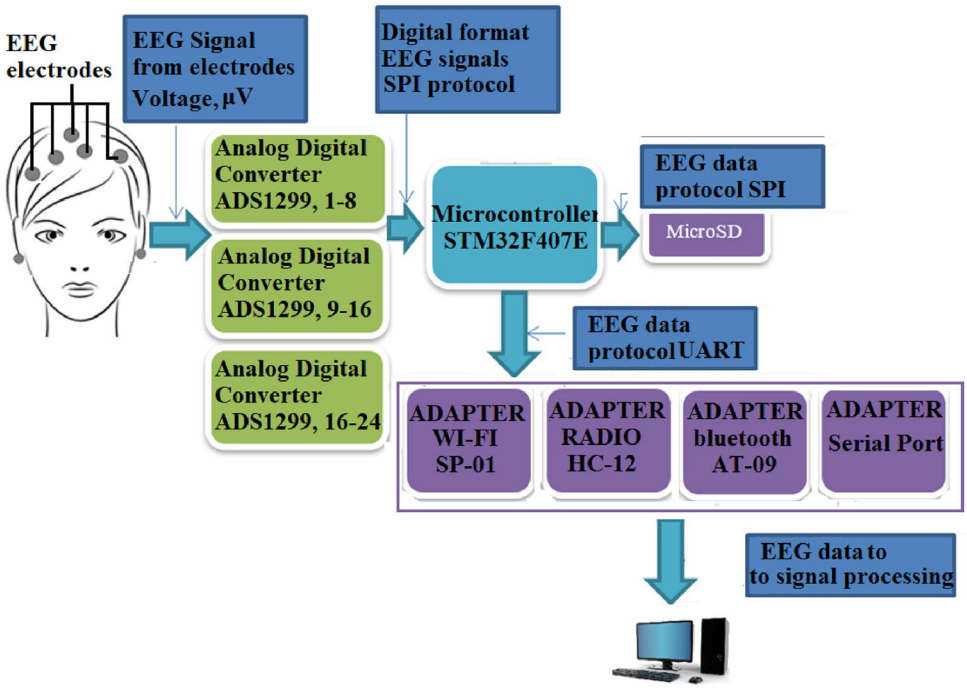

Fig. 1 Block diagram of the presented EEG device. Green cells indicate the board containing analog to digital converter components, the blue cells indicating the board containing the microcontroller and violet cells indicate peripheral devices

Materials and methods

Choice of microcontrollers

Despite being a central part of the EEG system due to the specifics of the task (measuring signals in microvolts), we assumed that the microcontroller does not highly affect the accuracy of our signal measurement. We could not find any evidence showing that one type of microcontroller introduces more electromagnetic interference into the EEG signal than another. As a result, the determining factor when choosing a controller was the availability of suitable peripherals. We selected the STM32F407VE microcontroller unit (MCU, referred to as stm32 for simplicity), which is based on the 32-bit ARMCortexM4 RISC core operating at a frequency of up to 168 MHz with 3 SPI ports, 2 I2C interfaces, and 2 UART ports.

Choice of analog to digital converter (ADC)

The ADC is one of the main elements in EEG recording, and the capabilities of BCI devices depends directly on it. There are not many ADC devices in the consumer market advertising specifically towards EEG research. The key factors for choosing our ADC were the input signal impedance, the ability to measure electrode impedance, and the potential to control the BIASout (Bias drive output). With these factors in mind, we chose the ADS1299 from Texas Instruments. Despite being a relatively old model, having been on the market for more than 10 years, the important difference between this ADC and the others is the presence of an internal multiplexer. The capabilities of this ADC and the characteristics of the multiplexer of ADS1299 were analyzed by Usman et al. (2018) and Deepshikha et al. (2015). The multiplexer allows us to control the internal settings of ADS1299 registers, granting us the ability to apply our own settings to each channel (gain, bias, measure impedance, etc.).

Choice of EEG processing software

The main objective of the software is to filter the signals from the noise, where the signal is decomposed primarily into frequencies corresponding to the brain's alpha (8–13 Hz), beta (14–40 Hz), theta (4–8 Hz), and delta (1–4 Hz) rhythms. In our research, we focused on the development of a hardware system, therefore we chose to use already available software for signal processing. When selecting software for EEG signal processing, it is necessary to consider the type of software license (proprietary or open source). For the low-cost segment, open-source software is ideal with the ability to freely access and make changes to the code. Of the well-known open-source options, OpenVibe is very popular. Mahmoodin et al. (2014) described the benefits of this library, including its open-source nature and ease of signal processing applications.

Other common free software includes:

- EEGLAB (https://sccn.ucsd.edu/eeglab/index.php)
- Fieldtrip (https://www.fieldtriptoolbox.org/)

- Brainstorm (https://neuroimage.usc.edu/brainstorm/)
- TAPEEG (https://sites.google.com/site/tapeeg/)
- sLORETA (http://neurofeedbackalliance.org/sloreta/)
- Brainflow (https://brainflow.readthedocs.io/en/stable/)

Of the paid options, popular software includes:

- BrainExpress (https://store.neurosky.com/products/brainexpress)
- BioEra (http://www.bioera.net/index.shtml)
- BrainZen (https://store.neurosky.com/products/brainzen)
- Neuromore (https://www.neuromore.com/)
- NeuroRT Studio (http://smartbci.com/)
- NeurOptimal (https://neuroptimal.com/)
- Turbo-BrainVoyager (https://www.brainvoyager.com/downloads/downloads.html)

As for Python libraries, the MNE library is one of the most popular options. Gramfort et al. (2013) analyzed this library and its ability to process EEG and MEG signals. Brainflow is a library designed to obtain, parse, and analyze EEG data using integrated devices that read the EEG signals. We chose BrainFlow for this project, partially due to its Timeflux plugin: an open-source framework for the acquisition and real-time processing of bio-signals (https://timeflux.io/). Currently, our board has been integrated under the name of "ironbci" into the Brainflow library. For those seeking to follow this work and develop similar low-cost devices, many of the options listed above may be sufficient, as the software decision is largely left to personal preference.

ADS1299: our implementation

Choice electronic parts for power supply

For the ADS1299's power supply, we chose to use a bipolar configuration. For the positive voltage, we used the following voltage regulators: t3042 Ultralow RMS Noise: 0.8µVRMS (10 Hz to 100 kHz) and Ultralow Spot Noise: $2\text{nV}/\sqrt{\text{Hz}}$ at 10 kHz. For the negative voltage, we used a lt3094 Ultralow RMS Noise: 0.8µVRMS (10 Hz to 100 kHz) and an Ultralow Spot Noise: $2.2\text{nV}/\sqrt{\text{Hz}}$ at 10 kHz. These parts were chosen due to our prioritization of low-noise components, a critical part of an EEG system.

Measurement of common-mode rejection ratio (CMRR)

CMRR is the ratio of differential gain (ADIFF) to common-mode gain (ACM). CMRR is fundamental to working with differential input circuitry. To measure the CMRR, we connected all channels, including the reference channel, to a 10 Hz, 40 mV DC sine wave (Audio Precision AP2700). We then calculated the CMRR as follows:

$$\text{CMRR} = 20\log_{10}\left(\frac{\text{Ad}}{\text{Acm}}\right)dB, \tag{1}$$

where Ad is the power of the ADC amplifier and Acm is the common mode gain (the peak output voltage/peak input voltage, or signal amplification factor). A nominal 1 mΩ resistor in the feedback path in parallel with a 1.5 nF capacitor provides a 100 Hz cutoff, which is wide enough to allow 50 Hz/60 Hz noise to pass through. Allowing this noise is necessary for our feedback system because if noise is present in the signal wire it must be present in the reference wire as well.

Measurement of signal-to-noise ratio (SNR)

Signal to noise ratio (SNR) is a dimensionless value equal to the ratio of the useful signal power to the noise power. This indicator is especially important for our device, since the noise is in the same microvolt range as the useful signal. This indicator was determined using the following formula:

$$\text{SNR} = \frac{P_{\text{signal}}}{\text{P}_{\text{noise}}} = 20\log_{10}\left(\frac{A_{\text{signal}}}{A_{\text{noise}}}\right), \tag{2}$$

where P is the average power for the useful signal and noise and A is the mean-square value of the amplitude for the useful signal and noise. A noise signal with a duration of 2 min was recorded on all channels of the ADS1299 at a sampling frequency of 250 Hz. Duration—duration of response to stimuli. If the voltage peak became 1.5 times larger, then they began to measure the time until the peak voltage again decreased. Average noise was calculated for all eight channels. The Audio Precision AP2700 generated a signal with a frequency of 20 Hz and an amplitude of 30 mV.

The DC gain of the BIAS amplifier was calculated by dividing the feedback resistor by a parallel combination of resistors connected to the summing junction. If 3 electrode inputs are selected for example, the gain would be calculated using the following formula, with M and K representing mega and kilo Ohms, respectively:

$$\text{Gain} = -\left(\frac{1M}{220K * 3}\right) = -13.63. \tag{3}$$

The value of amplifier outputs cannot be closer than 200 mV to the power supply. If the outputs of the amplifiers are within 200 mV of the supply rails, the amplifiers saturate and therefore become non-linear. To prevent this non-linearity, the output voltages must not exceed the common-mode range of the external interface.

Impedance measurement and common-mode interference

It is known that the impedances of EEG electrodes decrease over time due to the drying of electrode gel. These electrode connections must be constantly monitored to ensure a suitable connection. The basic method for measuring impedance at the interface between the electrode and skin is for the EEG system to inject a known current through the electrode and measure the resulting voltage difference. Since $V = I * R$, we can easily calculate the impedance. An internal excitation signal is used as a current source. This signal is generated by the settings defined in LOFF: Output Control Register. The available settings include Bits, FLEAD_OFF, initial frequency of the bit, and ILEAD_OFF. In our case, the impedance was 6 kOhm. During measurement, the ADS1299 monitored the skin impedance. We considered an increase in impedance by more than 200 kOhm during the test without conductive gel and 5 kOhm with conductive gel as an unacceptable impedance. Impedance was measured twice per minute, with results present in Table 3.

Our project uses 24 EEG electrodes, therefore several ADCs were needed in one circuit. To generate common mode signal, we closed the BIASINV pins together and turned off all but one of the BIAS amplifiers. This connected all the PGA outputs to one summing junction at the input of one BIAS amplifier (Fig. 2a). The internal scheme for BIASINV and BIASOut is presented in Fig. 2b, where the DC gain of the BIAS amplifier is calculated by dividing the feedback resistor by a parallel combination of resistors connected to the summing junction.

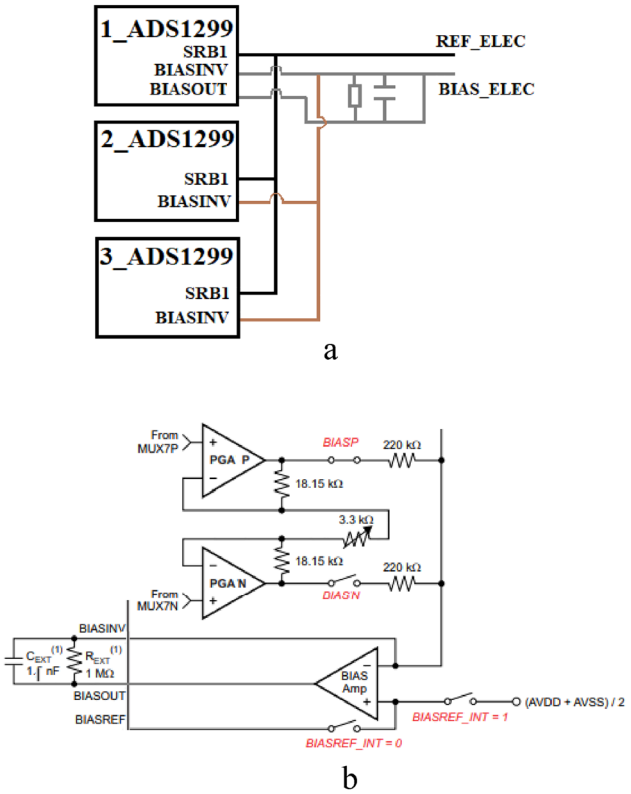

Fig. 2 Connecting multiple ADCs and internal scheme of ADS1299: **a** structural scheme, **b** internal scheme of ADS1299

Common-mode interference is interference on a transmission line, usually induced by an external source. Even though the influence of magnetic fields is not as critical for an EEG device as for magnetoencephalography (MEG), this perturbation can nevertheless introduce serious distortions into the measured signal. Arrubla et al. (2014) and Vorobyov et al. (1998) examined various electrical devices that emit different frequencies of electromagnetic fields and found that feedback was the simplest and most effective way of dealing with common-mode interference. Leske et al. (2019) and Urekar et al. (2017) described in detail the problem of the influence of external fields on the quality of the EEG signal, finding that it is imperative to keep the common-mode interference to a minimum. We used two methods to eliminate this interference: first by use of the ADS1299 which generates a BIASout signal, and second by exclusion of external machine fields incorporated in our device's design.

By means of BIASout, we maintained a constant voltage level within an acceptable range and minimized any common-mode AC signals in the body. To do this, BIASout relies on internal connections from the PGA outputs to BIASINV to complete the feedback loop. The device's housing, common-mode interference, stray characteristics of the cable, as well as the input signal circuit are all part of the feedback circuit of the BIAS amplifier, which allows us to suppress each of these interferences. The amplifier bias voltage was centered at 0 V (relative value), or rather the amplifier board's reference voltage (0 V level). BIASINV sets the feedback for adjusting the input voltage to BIASout. This is established by connecting the input signals from the electrode to BIASINV for the common-mode output. BIASref is the voltage reference for BIASout signal, which in our case was the internal reference voltage.

Special board construction for protection against an external magnetic field

First, to reduce the effect of external electromagnetic fields, the ADC boards are placed between two grounded metal plates. It is worth noting that in the low-cost market, many engineers miss this component and try to solve the problems with the influence of the magnetic field only through the bias electrode. Instead, we installed two grounded copper alloy plates between the ADC boards as well as using grounded coaxial cables with a characteristic impedance of 50 Ohm. We made special boards for connecting electrodes to coaxial cables through SMA connectors and placed further grounding plates between the boards (Fig. 3).

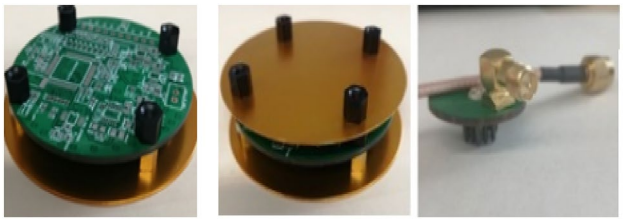

a b c

Fig. 3 Protection against an external magnetic field: **a**, **b** grounding shields between boards, **c** board with dry EEG electrode with the ability to connect a cable with grounding

Testing

Test parameters

ADS1299 internal noise check using a multiplexer

When measuring EEG signals, we followed the following safety and operational guidelines:

1. Medical electrical equipment—Part 2–26: particular requirements for the basic safety and essential performance of electroencephalographs
2. The standard (ANSI/AAMI) EC-12: 2000 standard for disposable electrodes.
3. Use of laboratory analyzers of impedance and amplitude-phase characteristics (In our testing we used a Solartron 1260 with a nominal accuracy of 0.1% from 5 ohms to 100 kOhms).
4. Noise measurements are made in accordance with the standard of medical equipment (EN 60601-1-2), which describes tests for resistance to power line frequency (50 Hz), tests for magnetic field (EN 61000-4-8) and tests for resistance to Radio Frequency (RF) emissions (EN 61000-4-3).
5. Before conducting any research, we verified:

- immunity to frequency (50 Hz) in the power line.
- immunity to radiation of radio frequencies.
- immunity to radiated radio frequencies.

To confirm proper operation of the power supply circuit and correct connection of the ADS1299 device, we checked the conformity of the noise by shorting the inputs of all channels through setting the ADS1299 register CHnSET = 1. Each measurement was carried out for 5 min, at a sampling frequency of 250 samples per second. The arithmetic mean values are presented in Table 1.

Table 1 Test results of internal noise for ADS1299

Output data rate	Noise (value from ADS1299 without nay transformation) (per gain setting in ADS1299)						
	1	2	4	6	8	12	24
16,000	140.1	268	500.1	800.1	934.4	1050.5	1304.9
8000	125.2	204.1	300.5	350.5	415.1	480.7	560.1
4000	115.1	145.4	160.6	178.1	190.1	194.1	200.1
2000	60.3	73.1	90.5	100.6	110.6	145.5	170.1
1000	32.1	45.7	68.1	76	91.9	120.6	152.6
500	4.3	7.1	8.9	10.4	23.1	35.6	46.7
250	1.1	1.5	2.2	2.4	4.7	6.7	10.7

Table 2 Test results of internal noise for ADS1299 with external different conditions

External different conditions	Value	Noise (value from ADS1299 without any transformation) (per gain setting in ADS1299)						
		1	2	4	6	8	12	24
Temperature, °C	15	1.05	1.2	1.9	2.8	5.1	5.9	11.1
	25	1.1	1.1	2.1	2.5	4.9	6.9	10.5
	40	1.5	1.5	2.5	2.9	5.7	7.5	15.9
Humidity, %	30	1.15	1.7	2.7	2.1	5.1	7.1	12.5
	60	1.05	1.8	2.6	2.2	5.1	7.2	12.6
	90	1.1	1.8	2.5	2.4	4.5	6.9	11.2
Electromagnetic fields, μT	1	1.3	2.1	2.2	2.5	4.9	6.1	12.1
	10	5.9	7.5	8.9	9.4	10.2	11.1	19.7
	30	6.1	11.1	22.8	25.14	44.7	56.7	81.4

Also, we tested the device with the same conditions under various external factors, such as different ambient temperatures, different humidity, and different electromagnetic field (Table 2).

As seen here, a rise in temperature increases the noise level, but thanks to temperature sensors (measured by SHT30-D) on the board we can try to compensate for this noise in the future. Humidity (measured by SHT30-D) does not affect the noise level. The larger the electromagnetic waves (measured by Mustool MT525), the greater the signal noise.

Referencing techniques for EEG recording are e.g., average reference (the mean voltage from all electrodes subtracted from the individual electrode) or separate referencing electrode/electrodes (the voltage from the reference electrode/electrodes subtracted from the individual electrode) reference electrode. Junghöfer et al (1999) in their work point out that when the number of electrodes is less than 64, it is not advisable to use the averaged reference. Therefore, in our case a separate electrode was used for the reference, fixed on the earlobe with a clamp. For the manufacturing of the board, we used typical fiberglass—FR4 with a nominal thickness of 1.6 mm, lined with 35 µm copper foil of both sides; HASL technology was used for the coating. The final board consists of three circular plates with a diameter of 50 mm each. The first board contains the power supply, with a 600 mAh LiPo battery attached for our tests. The battery voltage is 4.2 V, so the output of the board contains a step-up transformer to convert this voltage to 5 V. Then, from the power board, the power supply connects in parallel to the second board (containing the MCU) and the third board (containing the ADS1299). Figure 4 shows images of boards both blank and with soldered elements.

For measuring the EEG signal, we used electrodes from Florida Research Instruments Inc (https://www.fri-fl-shop.com/). It is important to use the same electrode metal for all electrodes, as this minimizes the risk of a galvanic effect (the occurrence of a contact potential difference when two conductors of a different metal are connected).

Assessment of chewing artifact

Before conducting this test, we measured the resting noise of our device to be 0.5 µV (Appendix 1). This value accords to the characteristics of ADS1299 listed in the manual.

Chewing and blinking are pronounced and well-studied artifacts in EEG signals. Therefore, they are often used for the process of checking the correct operation of an EEG device. Allen et al. (2014) and Pickworth et al. (1988) described in sufficient detail the process of recording and recognizing the chewing artifact on an EEG scan. There are many different methods to neutralize these artifacts, and

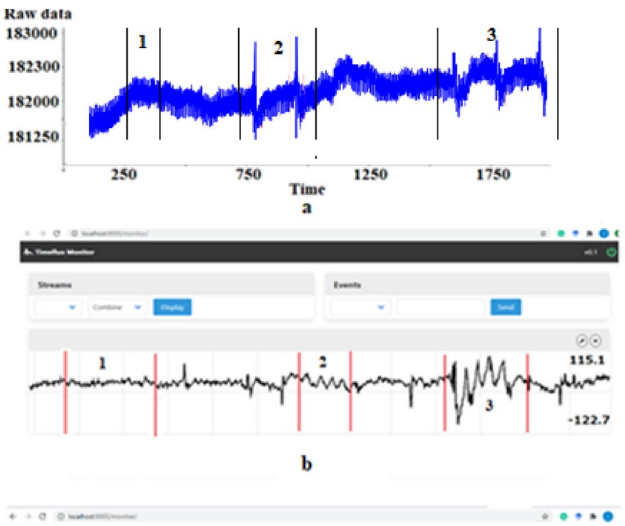

Fig. 5 Artifact test. **a** measurement process for the chewing artifact with dry electrodes. Chewing occurred in the following sequence: 1 time, 2 times, and 3 times. The Y axis is raw EEG signal. **b** blinking process with dry electrodes, where 1—eyes are closed, 2—blinking occurs four times and 3—chewing occurs four times, where the Y axis is µV post signal processing (using Timeflux software)

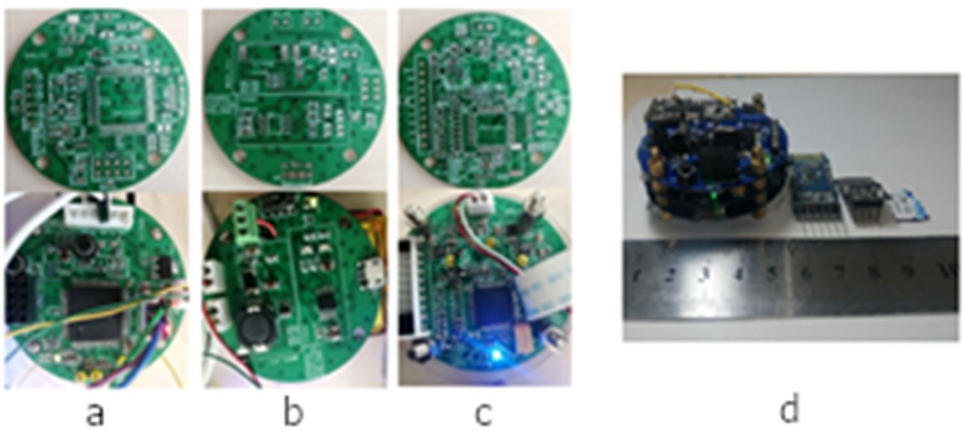

Fig. 4 General view of the device: **a** down microcontroller unit (MCU) board and upper blank for board, **b** down ADS board and upper blank for board, **c** down power supply board and upper blank for board, **d** a general view of the device with modules for transfer data by Radio, Wi-Fi, Bluetooth and micro SD card storage

Sheoran and Saini (2020) and Borowicz (2018) have detailed how to detect and how to deal with them. In our tests, the chewing and blinking artifacts, detected with an electrode placed at Cz, were very recognizable and completely coincided with expectations (Fig. 5).

Signal processing was performed with the Brainflow plugin Timeflux, with a band pass filter from 1 to 40 Hz (Fig. 5b). The measured noise was about 0.5 µV when the signal is closed with electrodes, and a slight network noise of about 0.05 µV was noticeable because of external magnetic fields affecting the cables.

Recordings of alpha rhythms

Alpha rhythm (α-rhythm) is the rhythm of the brain in the frequency band from 8 to 14 Hz with an average amplitude of 30–70 µV that serves as a popular method for validating an EEG recording system (Newson and Thiagarajan 2019). Often, these waves are recorded in an awake subject during relaxation, with their eyes closed, as described in detail by Pedrosa (2017). To detect alpha waves, we connected eight electrodes to points along the 10–20 electrode placement system (F3, F4, T3, Cz, T4, T5, T6, Pz) with four male subjects (age 25–35) and two female subjects (age 24–28). The recording was carried out for 30 s both when the eyes were open and when the eyes were closed. We observed an increase in activity in the frequency band of 8 to 14 Hz, which again is a typical alpha-rhythm signal in the occipital lobe of the brain. The frequency of the alpha rhythm is associated with cerebral blood flow and decreases with a reduction in blood supply to other parts of the brain. We observed a weakening of alpha activity when the eyes were opened, however when the eyes were closed alpha activity returned to its amplitude and frequency in the occipital region. The average amplitude of the alpha rhythm was near 100 µV. This behavior is a typical signal of the alpha rhythm in the occipital lobe of the brain. We averaged different signal characteristics during our 10 experiments and presented them in Table 3, looking for changes in alpha fluctuations in the current data in µV.

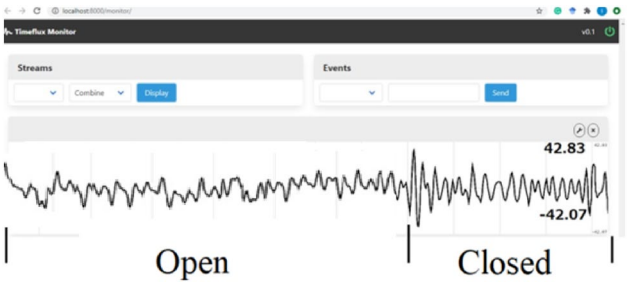

Fig. 6 EEG signal of alpha activity with open and closed eyes

Comparison of EEG signal (alpha activity) with closed eyes and with open eyes is shown in Fig. 6.

P300

The P300 is already a well-researched phenomenon, as it was discovered back in the mid-1960s by researchers Chapman and Bragdon (1964), who found that EEG signals correlate with visual stimuli of numbers and flashes of light after 300 ms. The use of this method has found wide application in the control of mechanical limbs and BCI spellers (akin to keyboards). Song (2020) used this phenomenon and obtained an accuracy of 94.43% in a stand-alone test with data for eight participants performing a mechanical arm control task.

To detect the P300 signal with our device, we connected eight electrodes from the 10–20 electrode placement system again to the same group of subjects mentioned in paragraph 3.3. We used the methodology presented by Ganin et al. (2013) where the stimulus was an increase in the brightness of a sphere on a computer monitor. The balls flashed in a random order, with no pauses between flashes. Only one ball blinked each time, so the paradigm was analogous to the mode of single-cell stimulus presentation in the static P300. We averaged different measured signal characteristics and presented them in Table 4. Amplitude increase in %—refers to the increase in amplitude relative to the baseline before stimulus presentation. Time refers to the response time and duration refers to the duration of the response.

Table 3 Averaged various signal characteristics during our experiments

Characteristics	Electrode location in according to international system of placement of electrodes "10–20" for dry electrodes							
	F3	F4	T3	Cz	T4	T5	T6	Pz
Measurement of common-mode rejection ratio CMRR, dB	110	115	110	117	110	110	112	111
Internal noise, µV	0.1	0.09	0.1	0.11	0.1	0.11	0.1	0.1
External noise, µV	0.3	0.25	0.4	0.3	0.32	0.35	0.26	0.3
Noise/ratio SNR, dB	124	122	125	125	123	126	126	124
Impedance	180	194	210	200	210	205	215	201

Table 4 Averaged various signal characteristics during our experiments

Characteristics	Electrode location in according to international system of placement of electrodes "10–20" for dry electrodes							
	F3	F4	T3	Cz	T4	T5	T6	Pz
Amplitude increase in %	110	150	120	140	90	120	130	100
Time, ms	290	310	295	305	340	310	290	300
Duration, ms	280	300	290	360	310	315	290	320

Standard error for the amplitude increase was 4%, 3.8% for time, and 4.1% for duration.

Discussion and conclusion

In this article, we presented in detail the results of testing the developed device. On our GitHub page, we provide detailed instructions and all necessary technical documentation that will allow anyone to built this EEG device. We successfully developed a device with a peak input noise of 0.5 µV and a common-mode signal rejection ratio of 110 dB in the 0–50 Hz band. This device can capture EEG signal from 8 to 24 channels with a sampling rate of 250–1000 Hz. Apart from the presence of an additional (and optional) sensor board, the main difference of this board from the comparable systems is low power consumption, high accuracy, and compactness, which allows easy, portable use for long periods of time without recharging (though power draw varies from 85 to 400 mA depending on the number of electrodes used). The addition of the sensor board to the system allows it to monitor the state of environment (temperature, humidity, and air quality), physiological activity (gyroscope and accelerometer), and speech activity (microphone) for use in future analyses. The sensors are made with MEMS technology, which makes it possible to install them compactly on one semi-circular board with a diameter of only 50 mm. The sensors are connected to the microcontroller using the I2C protocol, which can then wirelessly relay the information to the off-board computer using the same wireless connection the EEG signal is transmitted through. These sensors are designed to collect environment data which ultimately will allow us to determine the correlations between various external factors and measured EEG signal in a future study. This information, together with the mathematical filters that are implemented in the software, will ideally allow for very high-quality EEG signal acquisition.

In this manuscript, special attention is paid to combating common-mode noise. Noise suppression is carried out via specific hardware parts and heavily shielded cables. A Wi-Fi connection allows you to transfer data directly to an off-board computer that implements software signal filtering and recording/storage of the data. With a 600 mAh LiPo battery, the system can operate for up to 6 h with eight electrodes and WI-FI data transfer. The device is designed for continuous use and data collection, ideally for establishing larger datasets for the subsequent use of neural networks. Our goal was to get more enthusiasts involved in BCI development through open-source hardware and the overall low cost of the device. This will hopefully allow for a more open and easy collection and exchange of data online. The cost of this device is within $350 (for 24 electrodes), which is significantly lower compared to similar systems on the market, especially at this performance level. In Table 5, we present a comparison of our device with OpenBCI.

In the future, we plan to increase the operating time of the device through use of various modes available in our microcontroller, such as energy saving mode from stm32 and Low Power Run (LP Run). We also plan to move the filtering work to a processor with a higher bus bandwidth than the microcontroller.

As far as the contribution to BCIs, the proposed device fills an important gap left by the competitors on the market. As mentioned above, there is a lack of low-cost EEG

Table 5 Comparison between open-sources ironbci and OpenBCI

Name	Microcontroller	Channels	Resolutions (bits)	Cost, $	Communications	Noise, mkV
ironbci	STM32F407VE	24	24	350	Wi-Fi Radio Bluetooth Serial SD card	< 1
OpenBCI	PIC32MX250F	8	24	750	Wireless data transmission SD card	> 1 (Sullivan et al. 2019)

devices capable of producing research-grade signals. While analogs such as the Emotiv Epoc or Neurosky Mindwave headset may provide research-grade options in terms of the signal, they fall short in customizability with fixed electrode placement and limited channel counts. These are only a few examples, but the market at this price point is very sparse.

The proposed device provides an EEG system that can allow inexpensive and rapid prototyping of BCI setups without a massive overhead investment into an EEG system. The emphasis on portability is also important because, while many EEG systems are used in hospitals and labs, the end goal for BCI systems is to improve the quality of life for the patients. A portable, wireless, low-cost EEG system opens up massive potential for BCI designs that help individuals in common daily environments, not just in labs.

Future work

With EEG measurement in microvolts, there are many seemingly insignificant issues that ultimately can affect the measurements of EEG signals. These include the choice of gel, the choice of attachment method, methods implementing noise reduction, etc. Each of these components could add noise, which is difficult to assess and requires additional research. We plan to use the accessory sensor board to establish the correlation between EEG signals and external factors in future research.

Appendix 1

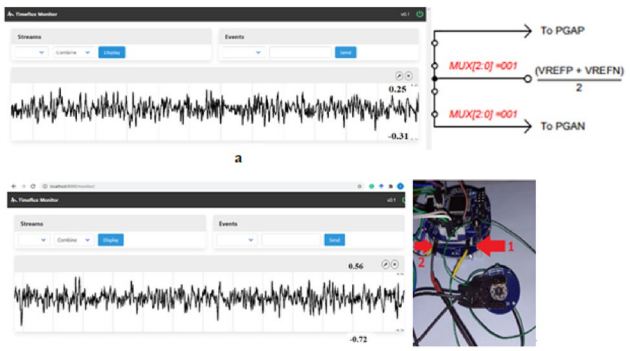

Noise test: **a** (left)—graph with process noise measurement where the electrode's input is shorted internally by register MUXn[2:0], shown schematically on the right; **b** (left) graph with process noise measurement where the reference signal and EEG signal are shorted by electrodes, shown on the right, where 1 indicates the cable from measurement electrode and 2 indicates the cable from the reference electrode.

Acknowledgements We would like to thank Pierre Clisson, an author of Timeflux open-source framework for the acquisition and real-time processing of biosignals.

We would also like to thank to Robert Oostenveld from Radboud University for his comments in the process of preparing this manuscript and to Sergey Stavisky from Stanford University for his advice on improving the quality of the manuscript.

We would like to express our gratitude to the anonymous reviewers for their helpful comments.

Declarations

Conflict of interest The authors declare no conflicts of interest. The funders had no role in the design of the study, in the collection, analyses or interpretation of data, in the writing of the manuscript, or in the decision to publish the results.

References

Allen A, Jacob T, Smith A (2014) Effects and after-effectsof chewing gum on vigilance, heart rate, EEG and mood. Physiol Behav 133:244–255

Arrubla J et al (2014) Methods for pulse artefact reduction: Experiences with EEG data recorded at 9.4T static magnetic field. J Neurosci Methods 232:110–117. https://doi.org/10.1016/j.jneumeth.2014.05.015

Asadzadeh S, Rezaii T, Beheshti S, Delpak A (2020) A systematic review of EEG source localization techniques and their applications on diagnosis of brain abnormalities. J Neurosci Methods 339:108740

Ashby C, Bhatia A, Tenoreb F, Vogelstein J (2011) Low-cost electroencephalogram (EEG) based authentication. Proceedings of the 5th international IEEE EMBS conference on neural engineering Cancun, Mexico, April 27–May 1, 2011, pp. 442–445

Borowicz A (2018) Using a multichannel Wiener filter to remove eye-blink artifacts from EEG data. Biomed Signal Process Control 45:246–255

Chapman R, Bragdon H (1964) Evoked responses to numerical and non-numerical visual stimuli while problem solving. Nature 203:1155–1157. https://doi.org/10.1038/2031155a0

Chatrian G, Lettich E, Nelson P (1985) Ten percent electrode system for topographic studies of spontaneous and evoked EEG activities. Am J EEG Technol 25:83–92

Chaudhary U, Birbaumer N, Ramos-Murguialday A (2016) Brain–computer interfaces for communication and rehabilitation. Nat Rev Neurol 12:513–525

Dadebayev D, Goh W, Tan E (2021) EEG-based emotion recognition: Review of commercial EEG devices and machine learning techniques. J King Saud Univ Comput Inf Sci. https://doi.org/10.1016/j.jksuci.2021.03.009

Deepshikha A, Asha R, Shivangi A (2015) EEG data acquisition circuit system Based on ADS1299EEG FE. 2015 4th International conference on reliability, infocom technologies and optimization (ICRITO) (trends and future directions). Doi: https://doi.org/10.1109/ICRITO.2015.7359346

Ganin P, Shishkin L, Kaplan A (2013) A P300-based brain-computer interface with stimuli on moving objects: four-session single-trial

and triple-trial tests with a game-like task design. PLoS ONE 8:10. https://doi.org/10.1371/journal.pone.0077755
Graham K (2014) Development of a compact, low-costwireless device for biopotential acquisition, Theses and Dissertations, Virginia Commonwealth University
Gramfort A, Larson E, Luessi M, Engemann D (2013) MEG and EEG data analysis with MNE-python. Front Neurosci 267:1–13
Gunawan A, Surya K (2018) Brainwave classification of visual stimuli based on low cost EEG spectrogram using DenseNet. Proced Comput Sci 135:128–139
Junghöfer M, Elbert T, Tucker D, Braun C (1999) The polar average reference effect: a bias in estimating the head surface integral in EEG recording. Clin Neurophysiol 110:1149–1155
Kanda A, Oliveira F, Fraga F (2017) EEG epochs with less alpha rhythm improve discrimination of mild Alzheimer's. Comput Methods Programs Biomed 138:13–22
Kübler A, Femke N, Birbaumer N (2007) Brain-computer interfaces for communication and motor control-perspectives on clinical applications. Toward Brain Comput Interfac 1:373–391
Leske S, Dalal S (2019) Reducing power line noise in EEG and MEG data via spectrum interpolation. Neuroimage 189:763–776
Lopez-Gordo M, Sanchez-Morillo D, Valle F (2014) Dry EEG electrodes. Sensors (basel) 14(7):12847–12870
Luis L, Gomez-Gil J (2012) Brain computer interfaces, a review. Sensors 12(2):1211–1279
Mahmoodin Z, Lee Y, Mansor W, Mohamad (2014) Processing of electroencephalogram signals using OpenVibe. Conference, 2014 IEEE Region Vol.10, pp. 563–567
Newson J, Thiagarajan T (2019) EEG frequency bands in psychiatric disorders: a review of resting state studies. Front Hum Neurosci. https://doi.org/10.3389/fnhum.2018.00521
Pedrosa P, Fiedler P, Schinaia L, Vasconcelos B (2017) Alginate-based hydrogels as an alternative to electrolytic gels for rapid EEG monitoring and easy cleaning procedures. Sens Actuators B Chem 247:273–283
Peterson V, Galván C, Hernández H, Spies R (2020) A feasibility study of a complete low-cost consumer-grade brain-computer interface system. Heliyo 6:3. https://doi.org/10.1016/j.heliyon.2020.e03425
Pickworth W, Herning R, Henningfield J (1988) Mecamylamine reduces some EEG effects of nicotine chewing gum in humans. Pharmacol Biochem Behav 30:149–153
Savadkoohi M, Oladunni T, Thompson L (2020) A machine learning approach to epileptic seizure prediction using Electroencephalogram (EEG) Signal. Biocybern Biomed Eng 40(3):1328–1341. https://doi.org/10.1016/j.bbe.2020.07.004
Senevirathna B, Berman L, Bertoni N, Pareschi F (2016) Low-cost mobile EEG for characterization of cortical auditory responses. IEEE Int Symp Circuits Syst (ISCAS) 1:1102–1105
Sheoran P, Saini J (2020) A new method for automatic electrooculogram and eye blink artifacts correction of eeg signals using CCA and NAPCT. Proced Comput Sci 167:1761–1770
Song Y et al (2020) A practical EEG-based human-machine interface to online control an upper-limb assist robot. Front Neurorobotics. https://doi.org/10.3389/fnbot.2020.00032
Sullivan M et al (2019) Analysis of a low-cost EEG monitoring system and dry electrodes toward clinical use in the neonatal ICU. Sensors 19:2637. https://doi.org/10.3390/s19112637
Tyler S, Leibbrandt S, Fitzgibbon S (2015) Measurement of neural signals from inexpensive, wireless and dry EEG systems. Physiol Meas 36(7):1469–1484
Tylová L, Kukal J, Hubata-Vacek V, Vyšata O (2018) Unbiased estimation of permutation entropy in EEG analysis for Alzheimer's disease classification. Biomed Signal Process Control 39:424–430
Uktveris T, Jusas V (2018) Development of a modular board for EEG signal acquisition. Sensors 18:2140
Urekar M, Sovilj P (2017) EEG dynamic noise floor measurement with stochastic flash A/D converter. Biomed Signal Process Control 38:337–345
Usman R, Imran K, Nada S, Denise T (2018) An EEG experimental study evaluating the performance of Texas instruments ADS1299. Sensors 18(11):3721. https://doi.org/10.3390/s18113721
Vorobyov V, Sosunov V, Kukushkin N (1998) Weak combined magnetic field affects basic and morphine-induced rat's EEG. Brain Res 781:182–187
Yu H, Lei X, Song Z, Wang J (2018) Functional brain connectivity in Alzheimer's disease: an EEG study based on permutation disalignment index. Phys A 506:1093–1103